Construction and Building Materials 408 (2023) 133781

Contents lists available at ScienceDirect

Construction and Building Materials

journal homepage: www.elsevier.com/locate/conbuildmat

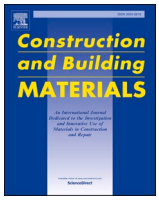

Improving the performance of recycled concrete by biodeposition of biogenic silica as a surface coating

Daniel Merino-Maldonado [a,*], Andrea Antolín-Rodríguez [a], Saúl Blanco [b], Julia Mª Morán-del Pozo [a], Julia García-González [a], Andrés Juan-Valdés [a]

[a] INMATECO RESEARCH GROUP (Engineering of Materials and Eco-efficiency), Department of Agricultural Engineering and Sciences, University of León, Spain
[b] Department of Biodiversity and Environmental Management, University of León, Spain

ARTICLE INFO

Keywords:
Surface treatment
Durability
Biodeposition
Diatoms
Biogenic silica
Construction and demolition waste (CDW)
Recycled concrete

ABSTRACT

This study addresses the challenges of sustainability and the implementation of a circular economy in the construction and maintenance of concrete structures used in clean-water applications. Specifically, it examines the use of an innovative surface treatment based on a biofilm comprising diatom biosilica deposition as a waterproofing agent and surface pore sealant to improve the longevity of recycled concrete. To this end biofilm-treated and untreated (control) samples of a concrete mix containing 50% recycled aggregates were subject to four performance tests directed at assessing the durability of concrete structures under environmental conditions: resistance to carbonation, freeze–thaw durability, resistance to water penetration, and electrical resistivity as an indicator of the corrosion resistance of concrete. In addition, the protective biofilm was characterised using SEM. Results suggest that the biogenic silica surface treatment significantly improves the durability of recycled concrete, in particular, for treated compared to untreated samples there was a 56 % reduction of the carbonation front, 26% lower mass loss in freeze–thaw cycles, 57% reduction in the water penetration front under pressure, and 44% higher electrical resistivity. Together these findings confirm that the biofilm used in this study constitutes an effective treatment to improve the properties of recycled concrete and ensure its durability, particularly when used in the construction of structures in contact with constant water fluctuations.

1. Introduction

Clean water infrastructure is fundamental to much of modern society. Irrigation canals and dams enable the management of key water resources for drinking-water, hydropower production, and flood protection, among other services. However, the construction and maintenance of this infrastructure requires vast amounts of concrete and this poses very particular issues [1,2].

The amount of concrete used in the construction of hydraulic infrastructure presents a major challenge in terms of sustainability and there is a need to move towards a more circular economy [3]. The production of cement, one of the main components of concrete, is highly energy intensive and is thus responsible for substantial greenhouse gas emissions. In addition, the extraction and processing of aggregates, which comprise up to 75 % of a typical concrete mix [4], have a significant environmental impact. This means that the concrete industry is a heavy consumer of natural resources and also a major source of environmental pollution [5].

In this context, it is essential for the concrete industry to move towards a more sustainable, circular economy in which greater use is made of recycled concrete. However, the quality of concrete made with recycled aggregates (RAs) is often poor. The heterogeneous nature of RAs results in concretes characterised by high porosity and thus hight water absorption [6], making the use of these concretes problematic in terms of their durability since water penetration can lead to a variety of structural defects that might compromise performance.

This said, some recent studies [7–10] have proposed the use of RAs as a substitute for natural aggregates (NAs) in the manufacture of concrete, with some supporting substitution percentages of more than 50 % [11–13]. In this way, experimental tests in the present work were completed using samples of a concrete mix in which 50 % of natural aggregates were substituted for RAs (50 % RA concrete). In addition, and of particular interest here, is a study investigating the use of concrete made with RAs specifically for use in the construction of hydraulic

* Corresponding author.
E-mail address: dmerm@unileon.es (D. Merino-Maldonado).

https://doi.org/10.1016/j.conbuildmat.2023.133781
Received 30 May 2023; Received in revised form 2 October 2023; Accepted 10 October 2023
Available online 18 October 2023

infrastructure [14].

However, to increase the use of recycled concrete, perhaps the most important area of research is the development of techniques to improve its strength and durability. In this regard, there is a growing number of surface pore-blocking treatment materials available to protect cement-based structure [15], which not only increase wear resistance but also reduce water permeability [16]. In addition, several studies have shown the effectiveness of laboratory-synthesised siliceous surface treatments [17–24], such as silane, silicates and Nano-SiO_2. These compounds act primarily as waterproofing agents due to their hydrophobic characteristics and have also been proven to reduce the size of concrete surface pores so reducing water absorption capacity [25].

In this way, the work presented here concerns the use a silica-based surface treatment was chosen for the present research; however, the silica compounds used here are of biological rather than synthetic origin. Specifically, biogenic silica produced by diatom deposition will be investigated as a as a cheap and natural alternative to synthetic silica treatments used to protect recycled concrete.

Diatoms are unicellular microalgae protected by a hard cell wall known as a frustule. These frustules consist almost entirely of hydrated silica (SiO_2) and possess unique mechanical and chemical properties [26]. Globally, diatoms are responsible for the majority of all bio-silicification making them the world's largest producers of biogenic silica and, in the process, they create the greatest variety of silicified structures of any living organism [27].

Despite the proven effectiveness of silica-based surface treatments in the protection of concrete, the clear potential of diatoms as a natural source for such coatings has not yet been explored. Indeed, to our knowledge, the only previous application of diatoms the construction industry is as the source of a self-cleaning coating for glass, ceramics, and glass ceramics [28]. This paper addresses this gap in the literature by evaluating the effectiveness of diatom bio-silica deposition as a protective surface treatment for recycled concrete exposed to the main agents of concrete deterioration.

If this biological treatment is proven to be effective, this could have significant implications for the construction and management of concrete structures used in clean-water applications. Because, it could provide a way of improving the longevity of recycled concrete allowing its more wide-spread use in hydraulic applications with significantly less environmental impact than the use of conventionally produced concrete.

2. Materials and methods

2.1. Materials

2.1.1. Concrete

The components of concrete mix used for this study are detailed on Table 1. The cement used was a blast furnace slag cement (CEM Type III/A 42.5 N/SR) manufactured without chemical additives and compliant with EN 197-1:2011 [29] in terms of physical, chemical, and mechanical properties. The proportion of coarse aggregates is calculated on the basis of previous research which has shown that the substitution of 50 % by these RA used in this study does not affect the properties of the concrete [30,31]. Thus, the coarse aggregates in this study are composed of 50:50 mix of natural aggregates (siliceous river gravel) and recycled aggregates (residual concrete, supplied by the CDW management company Valdearcos S.L.), while the fine aggregates comprised 100 % natural siliceous sand. To achieve a plastic consistency for the mix, a water-cement ratio of 0.59 was used.

Table 1
Components of Recycled Concrete Mix.

Components	RA	NA	Sand	Cement	Water
Dosage (kg/m^3)	585.5	585.5	642	354	210

Aggregates were characterized using the standard tests recommended in EN 933-1:2012 [32] and EN 1097-6:2014 [33], specifically those measuring particle density and water absorption after 24 h (WA_{24}). Table 2 shows the results for the three types of aggregate used, including coarse aggregates (RA: residual concrete with a grain size of 4–12.5 mm and NA: river siliceous gravel with a grain size of 4–12.5 mm) and fine aggregates (natural siliceous sand with a grain size of 0–4 mm). However, the particle size distribution of these materials is shown in Fig. 1, following the protocol of EN 933-1:2012 [32].

It is important to note that all the aggregates used in this study met the requirements of the European standard EN 12620:2003 + A1 [34]. However, due to the higher water absorption of the RAs [35], and given that they represented a high percentage of the mix used, their specific composition was investigated in more detail. This was done using the standard test described in EN 933-11:2009 [36], which assesses proportions of various materials in the aggregate: concrete, natural stone, gypsum and impurities, bricks and tiles, bituminous material, glass, and floating particles. The results are shown in Fig. 2.

After mixing, the concrete was poured into steel specimen moulds which were cured for 28 days at 20 ± 2 °C with a relative humidity of 100 %.

2.1.2. Diatoms

This research considers diatom biodeposition as a biological surface treatment for the protection of concrete structures. This biodeposition, in the form of biogenic silica [27], involves the adhesion of diatom frustules to the concrete surface to form a biofilm. These biofilms tend to be composed mainly of motile diatoms and adhesive extracellular polymeric substances (EPS) [37].

To generate the protective biofilm for study here, concrete samples were immersed in a test pond; all in the same region of the pond and to the same depth. The biofilm was allowed to develop over a specific period of time, after which, samples were removed and prepared for testing.

To quantify the diatoms present in the biofilm a measurement was made of the chlorophyll concentration (in μg Chla/mm^2) in films grown on four concrete specimens each measuring 100×100×100 mm. The average chlorophyll concentration was found to be 2.82×10^{-5} μg Chla/mm^2, which, multiplied by specimen surface area gives an value for the quantity of diatoms present in the biofilm.

The biofilms were further characterised in terms of, on one hand, diatom guilds and on the other, the proportions of desiccation-resistant species present, as shown in Fig. 3.

Diatoms form ecological guilds with other lifeforms depending on their preferred climactic conditions and feeding habits. The diatoms found in the biofilms grown for this research belonged to three main guilds (see Fig. 3a): epontic (living on the surface of the water), benthic (living on the bottom) and epontic and benthic (those that can live both on the surface and the bottom).

Hydraulic structures will be subject to fluctuations in water level, thus, for these biofilms to provide effective protection for these structures the diatoms of which they are formed must have some resistant to desiccation. There are two principal groups of diatoms: aerophilic diatoms, which can survive in dry environments with water level fluctuations, and aquatic diatoms, which are found in aquatic habitats and cannot survive in dry environments due to their delicate cell walls. Referring to Fig. 3b, analysis of the biofilm's diatom communities

Table 2
Aggregate Characterisation.

Aggregate	RA	NA	Sand
Fraction (mm)	4–12.5	4–12.5	0–4
D/d Ratio	3.33	2.66	6.65
Density ρ_p (Mg/m^3)	2.54	2.63	2.55
WA_{24} (%)	4.8	4.3	1.7

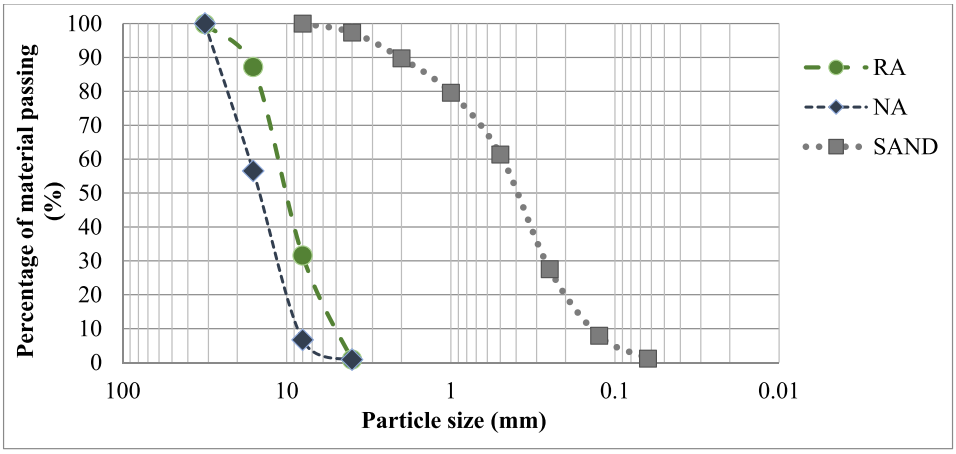

Fig. 1. Particle size distribution of aggregates.

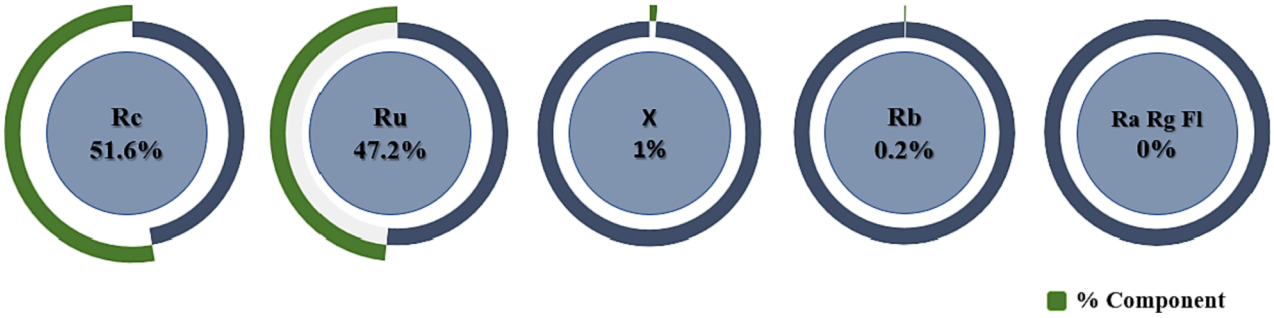

Fig. 2. Composition of Recycled Aggregates. Rc (Concrete); Ru (Natural Stone); X (Gypsum and Impurities); Rb (Bricks and Tiles); Ra (Bituminous Material); Rg (glass); Fl (Floating Particles).

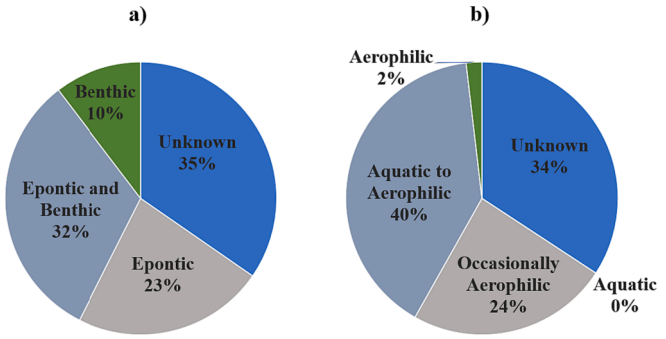

Fig. 3. Diatom characterisation. a) Diatom Guilds and b) Proportions of Desiccation Resistant Diatoms.

showed an almost complete absence of exclusively aquatic species with the majority belonging to a group of aquatic-to-aerophilic diatoms, that is, species that are nominally aquatic but are able to survive in dry conditions. The intended applications for the concrete under investigation here include structures that may experience varying levels of water coverage and indeed, may be completely dry for certain periods of time. Thus, the finding that these biofilms are robust to a certain degree of desiccation is important.

2.2. Methods

2.2.1. Concrete surface treatment

Four standard durability and one mechanical strength tests were used to evaluate the performance of the biofilm-protected concrete under the main environmental stresses to which hydraulic structures are routinely exposed. As specified in the respective standard, each test required concrete samples of a particular geometry. In this way, 6 different specimen geometries were necessary, each produced using a specially designed mould. Table 3 identifies the six tests completed and the specimen geometry (dimensions and cross-section of the test surface) required in each case.

Precautions were taken to ensure the test face (for biodeposition) of every specimen was as flat as possible. Concrete specimens were cured for 28 days, after which they were immersed in the test pond for 3 months. The test pond is located on the campus of the Environmental Institute of the University of León, in León (Spain), at an altitude of 828 m above sea level. Concrete specimens were subject to natural environmental conditions and no additional nutrients were provided to assist diatom growth.

Differing environmental conditions across the test pond might favour different diatom communities, thus, all specimens were placed within a

Table 3
Tests and Specimen geometries.

Tests	Number of samples	Dimensions (mm)	Test Surface (mm^2)	Biodeposition Per Specimen (μg Chla/mm^2)
Compressive	6	100x200	$\pi x50^2$	$5.56x10^2$
Carbonation	18	100x100x100	100x100	$28.20x10^2$
Freeze–Thaw Cycles	6	100x50	$\pi x50^2$	$5.56x10^2$
Water Under Pressure	6	150x300	$\pi x75^2$	$12.46x10^2$
Resistivity 1	6	400x100x100	100x100	$28.20x10^2$
Resistivity 2	6	75x150	$\pi x50^2$	$5.56x10^2$

specific area of the test pond to minimise variations in the biofilm growth. Specimens were submerged to a depth of 20 ± 5 cm below the water surface, that is, in the photic zone, with the test area of each specimen uppermost and oriented parallel to the water surface to encourage natural microalgae growth on the top surface of the concrete.

A range of environmental factors can limit the optimal development of diatoms [38]. These factors include temperature and the number of daylight hours, thus, to encourage biofilm growth, the emersion period chosen for the specimens was the three months coinciding with the spring equinox in the northern hemisphere (April to June). Due to the exponential increase in the number of daylight hours at this time of year, it is known as the positive photoperiod [39] and it is the optimal period for diatom growth.

During the period of study, climatic data were recorded including solar radiation levels and ambient temperature (see Fig. 4). It was calculated that over the whole of the three-month biofilm growth period, diatoms were exposed to a total of 1204.6 h of sunlight and experienced a mean temperature of 14,5 °C.

It has been demonstrated mature diatom colonies can be established on artificial substrates in only four weeks [39]. However, the density of the resulting biofilms was found to be low. For this reason, a minimum diatom growth period of three months was selected to ensure that experimental biofilms had adequate levels of silica biodeposition.

At the end of the biofilm growth period, the specimens were removed from the test pond and dried in a laboratory environment at a controlled temperature of 20 ± 2 °C with a relative humidity of 45 % ± 10 % for seven days.

During the three-month biofilm growth period, untreated control samples were prepared for comparison to biofilm-treated concrete. Once cured, these specimens were immersed in covered, light-tight water tanks to prevent the growth of any biological material. After three months, samples were removed from the water and dried under the same conditions as the biofilm-treated samples.

2.2.2. Analysis of biogenic silica and surface microstructure

Chlorophyll concentration was used as a quantitative measure of biofilm deposition. In this way, chlorophyll *a* was extracted from filtered GF/F samples with 90 % ethanol and its concentration was measured spectrophotometrically according to ISO 10260:1992 [40].

In order to study the diatoms themselves, samples were taken from the experimental substrates following the protocol of EN 13946:2014 [41], adapted for use in lentic systems. First, a brush was used to collect samples of epilithon from selected substrates (free from sediment and macroalgae) in the photic zone at several locations in the test pond. These samples were combined and preserved in a single 50 ml vial with formaldehyde (4 % v/v).

In order to examine the diatom frustules, it was necessary to make a clean suspension free of organic matter. To this end, hydrogen peroxide (120 vols.) was added to the preserved sample of epilithon and the resulting mixture was kept at 90 °C for 3 h to dissolve all organic matter. The sample was then centrifuged and decanted several times to obtain the desired suspension. Finally, drops of the suspension were mounted on slides for microscopic examination using a high refractive index synthetic resin.

The slides were analysed using a brightfield photomicroscope with a phase contrast condenser at 1000x magnification. The procedures established in EN 14407:2015 [42] were employed to quantify and identify diatoms. On each slide, a minimum of 400 individuals were identified to the highest possible taxonomic level, following Hofmann et al. [43] and their sources. The trophic indices of diatoms in each sample were calculated using OMNIDIA v.4.2 [44], a statistical programme developed for this purpose. These indices represent the ecological profile and preferences of each taxon.

Surface fragments from biofilm-treated and untreated specimens were coated with a 10 nm thick carbon layer using a high vacuum modular metallisation system (QUORUM Q150T ES). These samples were then examined under SEM in order to characterise surface morphology. The SEM used was a MERLIN microscope (Carl Zeiss), operating at 20 kV, equipped with a Bruker energy dispersive X-ray analyser (EDX), to provide additional information on the chemical composition of samples.

2.2.3. Compressive test on hardened concrete

Hardened concrete samples were subject to standard compressive strength tests as detailed in EN 12390–3:2020 [45] cylindrical specimens (Ø 100x200 mm) were used for this purpose: three biofilm-treated and three controls.

2.2.4. Durability test

The three the main agents of environmental damage affecting the durability of concrete include carbonation, freeze–thaw cycles, and water penetration. In this way concrete samples underwent tests to assess their resistance to these factors. Additionally, samples were subject to two resistivity tests to obtain an overall understanding of their corrosion resistance.

2.2.4.1. Carbonation resistance at atmospheric levels of carbon dioxide.

Standard test EN 12390-10:2019 [46] was employed using cubic specimens measuring 100×100×100 mm: nine biofilm-treated (D-samples) and nine controls (C-samples). Samples were cured for 28 days and after biodepositon which they were placed outdoors in a natural exposure site (León, Spain) with no direct rainwater contact to allow free air

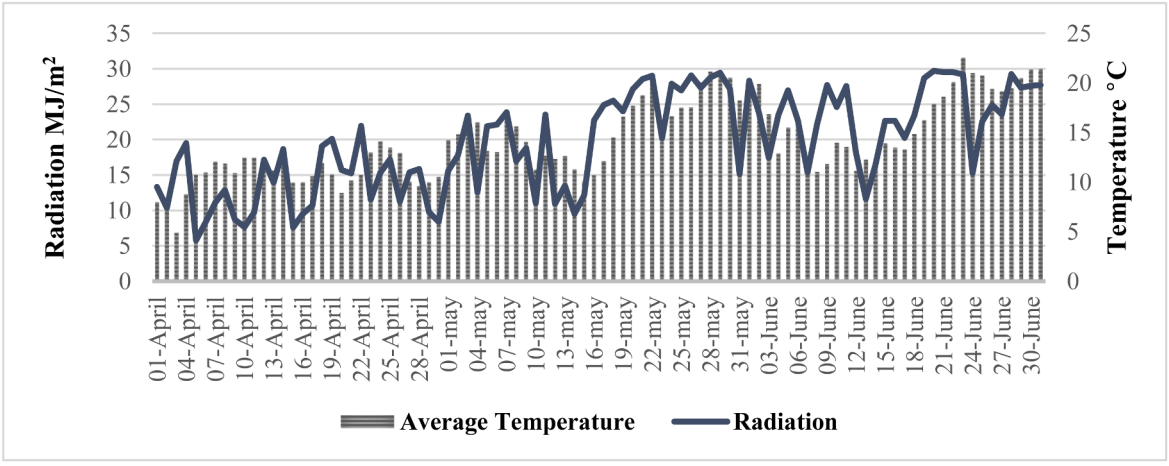

Fig. 4. External Environmental Factors.

circulation across the test surfaces.

The depth of carbonation in biofilm-treated and control samples was measured at three, six and twelve months. To identify the penetration front, the samples were split by traction perpendicular to the test surface, thus obtaining two subsamples. The presence of CO_2 within the concrete matrix (carbonation) results in physical–chemical processes leading to a reduction in pH [47], thus samples were sprayed with a phenolphthalein indicator to enable the observation of the carbonation front and measurement of its depth (d_k).

Standard tests require measurement of the carbonation front on all surfaces, however, for this purpose, only CO2 penetration through the test surface was evaluated. To obtain more accurate results, cross-sections were taken at 25 mm, 37.5 mm, 50 mm, 62.5 mm and 75 mm of each of the two subsamples (calliper accuracy = ±0.01 mm). An average was then taken of the penetration depth recorded for all 10 cross-sections.

Two alternative methods were used to calculate the carbonation rate, kc where the penetration depth, dk (mm), is related to the square root of exposure time in years ($\sqrt{}$years) as:

$$d_k = k_c.\sqrt{t} \quad (1)$$

In this way, an average value of k_c for the whole twelve-month test period can be found by plotting $\sqrt{}$(time in years) against penetration depth (mm). The method of squares can then be used to fit a line to the data points where the gradient of this line gives the value k_c. Alternatively individual values of k_c at three, six, and twelve months can be found by substituting values into Eq. (1).

2.2.4.2. Resistance of concrete to freeze–thaw cycles. Standard test EN-1339-Annex D [48] was employed using cylindrical specimens of Ø 100x50 mm: three biofilm-treated (D-samples) and three controls (C-samples).

Samples were conditioned and sealed into a lidded test vessel in contact with the test liquid (3 % NaCl saline solution) to a depth of 5 ± 2 mm. The test vessel was lined with a 0.035 W/(mK) elastomeric foam rubber thermal insulator, as specified in the standard [48] and with the lid in place, this provided a perfect air-tight seal.

Although it is recommended to remove scaling at regular intervals during the 28 freeze–thaw cycles, it was decided it would be sufficient to remove scaling only at the end of the process. Thus, after the 28 cycles, test surfaces were washed with water to remove any scaling. This solution was passed through a filter paper and the scaled material collected was then dried in an oven at 60 °C for 72 h after which it was weighed to determine the mass loss per unit area (kg/m^2).

2.2.4.3. Depth of water penetration. This test was performed in a compressed air driven water penetration tester (product number 270200: Mecánica Científica S.A, Madrid, Spain) and completed according to EN 12390–8:2020 [49].

As required by the standard, six cylindrical specimens of Ø 150x300 mm were subjected to a hydrostatic pressure of 5 bar (0.5 MPa), for a period of 72 ± 2 h. After 72 ± 2 h, the samples were subjected to a tensile force in order to split samples perpendicular to the test surface, so obtaining two half-sections from which to measure the water penetration depth (EN 12390–6:2010 [50]).

Analysis of the water penetration front requires two key measurements: P_{max}, the maximum depth of penetration and Pm, the average depth of penetration across the entire test surface. P_{max} was measured directly while P_m was calculated by dividing the area of the penetration front in mm^2 (obtained with ImageJ software [51]) by the sample diameter in mm.

2.2.4.4. Resistivity. Tests were completed according to standard EN 83988-1:2008 [52]. In these tests, AC current is supplied to two steel plate electrodes attached to the ends of a uniform cross-section sample of concrete. To ensure electrical contact between the electrodes and the concrete, prior to testing, specimens were saturated in water and superficially dried with a damp cloth and moist sponges (4 mm thick) placed between the electrodes and the concrete surface. In addition, the electrodes were insulated from supporting surfaces using wooden blocks which also ensured full, even contact between the electrodes and the concrete surfaces.

Two resistivity tests were completed using two distinct specimen geometries: six cubic specimens of 100x100x400 mm and six cylindrical specimens of Ø 100x200 mm. In each case, 3 biofilm-treated (D-samples) and 3 control samples (C-samples) were tested.

Current, I (Amps), through and voltage, V (Volts), across the concrete samples were measured and use to determine sample resistance, R_e (Ω). This value was used to find sample resistivity, ρ_e (Ω.m), using Eq. (2).

$$\rho_e = k.R_e \quad (2)$$

where k is the cell constant defined as sample cross section divided by its length.

3. Results and discussion

3.1. Compressive test on hardened concrete

The results of the compressive strength test are presented in Table 4. The compressive strength of the control samples (C-samples) is 31.30 MPa which is in line with other values recorded for concrete with the same replacement percentage of recycled aggregates (50 %). For example, a review by J. Kim [10] found a value of 29.3 MPa for concrete made using 50 % replacement with high quality recycled aggregates. In this way, our value seems a suitable reference and suggests that the aggregates used for the concrete examined here can be considered high quality.

The compressive strength of biofilm-treated concrete (D-samples) is 34.17 MPa. This shows that the biodeposition process does not result in deterioration of the concrete, on the contrary, treated samples are, on average, 9 % stronger than control samples. This small increase in compressive strength is surprising as the thin layer of biodeposited silica would not be expected to have a significant impact on the mechanical strength of the concrete. However, results of other studies have shown a similar phenomenon, for instance, work by Shirzadi Javid et al. [53] demonstrated a 4.4 % increase in compressive strength for concrete samples sprayed with a layer of Nano-SiO_2 compared to untreated samples, due to the increased density of the matrix on the surface of the concrete provided by the nanosilica.

3.2. Carbonation resistance at atmospheric levels of carbon dioxide

The results of tests for carbonation at atmospheric levels of carbon dioxide are shown in Fig. 5, The increase in the carbonation penetration front (d_k) over one year can clearly be seen in both C- and D-samples, however, it is considerably less pronounced in the latter indicating an increase in resistance to CO_2 permeability due to the biodeposition treatment. In addition, the depth of carbonation penetration in the D-samples is consistent throughout the test period: depth of penetration in C-samples is 56 % greater than for D-samples at six and twelve months, and it is only a few percent at 3 months.

Further evidence for the effectiveness of diatom biodeposition in reducing the CO_2 permeability of concrete was provided by calculations

Table 4
Compressive Test Results.

Samples	Compressive strength (MPa)
C-Sample	31.30
D-Sample	34.17

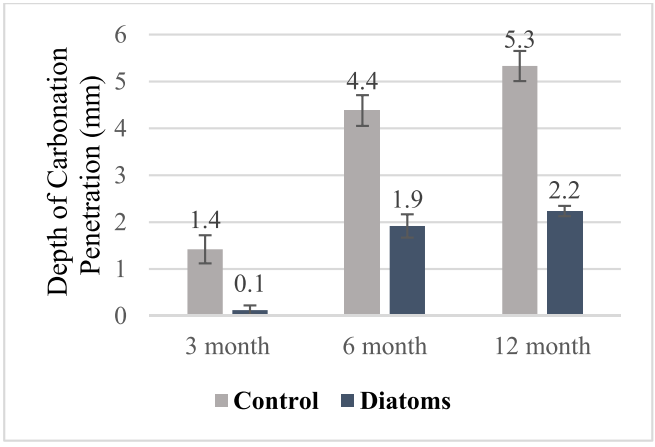

Fig. 5. Depth of carbonation penetration measured at three-month intervals over one year.

of the carbonation rate, k_c. The carbonation rate was determined in two ways. Firstly, average penetration depth (mm) was plotted against the square root of time elapsed in years ($\sqrt{}$years) to give a straight line graph of slope equal to k_c (Fig. 6a), and secondly, using Eq. (1) and substituting in average values for k_c after each time period (Fig. 6b).

The slope of the graph in Fig. 6a gives k_c = 2.43 mm/$\sqrt{}$years for D-samples compared to k_c = 5.63 mm/$\sqrt{}$years for C-samples demonstrating that bio-deposition reduces carbonation velocity by 57 %. Fig. 6b confirms these results showing a decreased value of k_c for D-samples compared to C-samples after each of the time intervals examined. The particularly high values of k_c (for both C- and D-samples) after 6 months ($\sqrt{t}$ = 0.71) can be attributed to the fact that this period coincided with the winter months and thus climactic conditions were particularly unfavourable (high humidity and low temperature). High humidity is especially problematic as carbonation rates tend to rise with increased humidity reaching a peak at 60–70 % humidity [54].

Several other studies have considered the effect of silicon-based surface treatments (silane or Nano-SiO_2) to reduce carbonation in concrete. For example, Zhu et al.[17] demonstrated a 50 % reduction in carbonation after application of a surface layer of silane (200 g/m^2) to concrete made with 100 % substitution with RAs. Similarly, Xia et al. [22] obtained promising results in their study concerning cement treated using colloidal Nano-SiO_2 with a particle size of 20 nm at 30 % concentration. However, not all studies show improvements with surface treatments, for example, Franzoni et al. [18] used 15.4 % colloidal Nano-SiO_2 with a particle size of 100 nm diluted in water (1:4) but found this to be ineffective in reducing carbonation.

The varying success of concrete surface treatments in reducing carbonation could be down to several factors. Firstly, concrete carbonation has been shown to be related to pore shape and pore connectivity, with larger pores allowing greater penetration of carbon dioxide [55]. Secondly, silica concentration and particle size will influence the pore-sealing ability of a given surface treatment [20]. In this way, the combination of concrete porosity and surface treatment characteristics must both be taken into account to find an effective treatment to combat carbonation.

3.3. Resistance of concrete to freeze–thaw cycles

If water penetrates the structure of concrete through surface pores, ice formation (specifically the outward pressure exerted as water expands on crystallisation) within the concrete matrix can cause structural damage [56] and this can be exacerbated by repeated freezing and defrosting in the presence of de-icers such as salt [23]. Typically, the freeze–thaw cycle will lead to loss of cement surrounding course aggregate particles resulting in surface scaling. In this way, mass loss due to frost damage can be used as a measure of a particular concrete's resistance to the freeze–thaw cycle. Fig. 7 compares mass loss in C- and D-samples (kg/m^2) after 28 freeze–thaw cycles and demonstrates that the latter have the lowest mass loss of the two types of samples. Indeed, biodeposition appears to increase the freeze–thaw resistance of concrete by 26 % compared to the untreated concrete.

The improved frost resistance observed for D-samples suggests that the growth of the biofilm blocks or reduces the size and connectivity of the pores in the concrete surface which limits the entry of water thus precluding the growth of ice crystals that would otherwise damage the concrete structure.

The results presented here are in line with those of several other studies, particularly that of Sakr & Bassuoni [21] who demonstrated a reduction in mass loss due to frost damage by 90–100 % compared to the reference samples using a surface treatment comprising colloidal Nano-SiO_2 of particle size of 50 nm at 25 % and 50 % concentrations. Similarly, Li et al. [23] showed that three layers of colloidal Nano-SiO_2 with a 10 nm particle size at 12.5 % concentration applied to concrete

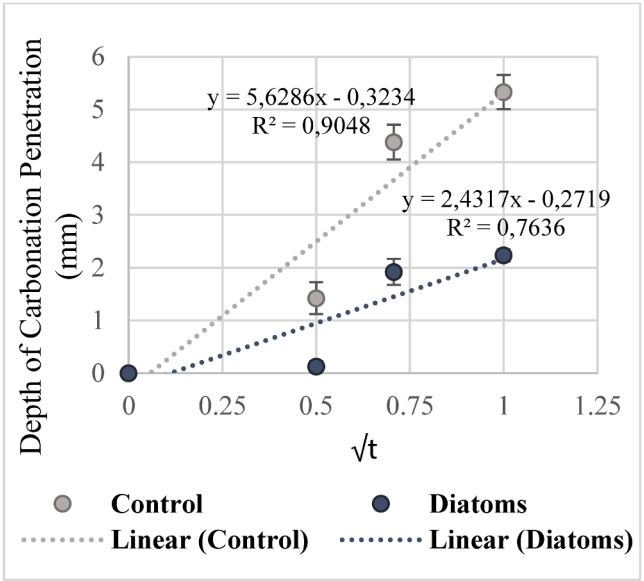

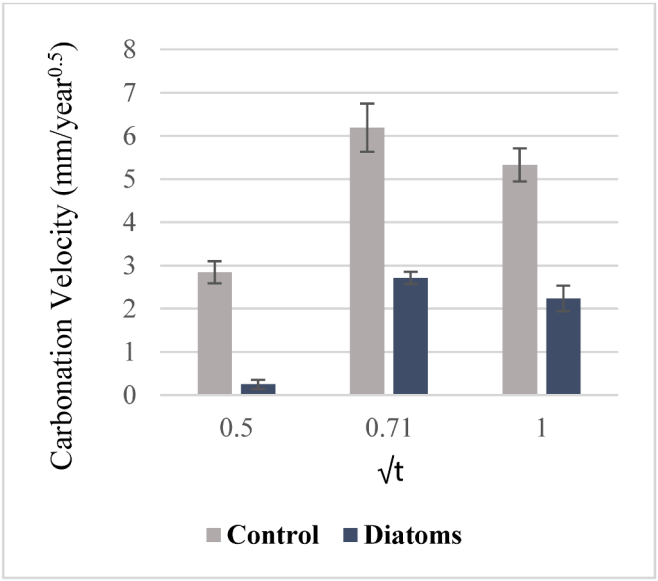

Fig. 6. Carbonation Velocity k_c Of the Samples. a) Total Carbonation Velocity and b) Carbonation Velocity in Different Periods.

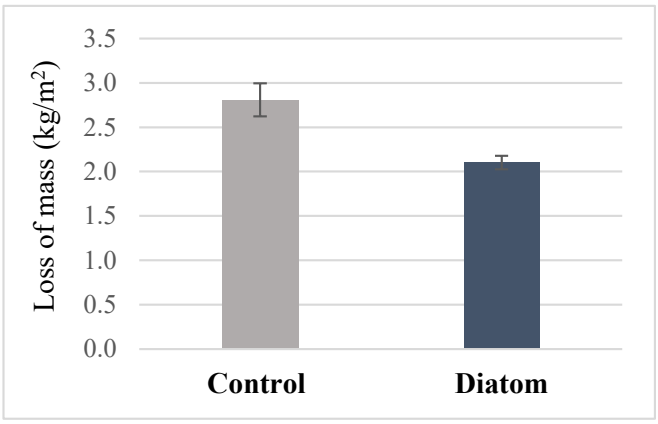

Fig. 7. Mass loss after 28 freeze–thaw cycles: untreated (C-samples) and biofilm-treated (D-samples) compared.

improved its frost resistance by 50 %, while Liu & Hansen [57] demonstrated that the application of 40 % silane almost completely eliminated mass loss after 80 freeze–thaw cycles.

3.4. Depth of water penetration

Results show that biofilm-treated D-samples suffer less water penetration than untreated C-samples both in terms of maximum water penetration depth (P_{max}) and average water penetration depth (P_m) as can be seen on Fig. 8.

In fact, the maximum water penetration depth for D-samples is 37 % less than that measured for C-samples while average water penetration depth is 57 % less for D-samples compared to C-samples. Thus, it would seem that biodeposition provides not only a limiting barrier to water penetration but is also a highly effective overall surface sealant. The difference between the maximum and average water penetration depths (Fig. 8), could be due to the fact that, as biological process, the deposition of diatom frustules does not result in a uniform film across the concrete surface. Anomalously thin areas of the film could then result in the recording of very high maximum penetration depths unrepresentative of the overall quality of the film. In this way, average penetration depth should be regarded as the more informative measure of biofilm effectiveness.

Similar results have been found in other work concerning silica-based coatings for concrete. For example, Ardalan et al. [58] reduced water penetration by up to 30 % with the application of a 50 % colloidal Nano-SiO_2 (particle size of 50 nm) film, while Li et al. [23] achieved a 43 % reduction of the water penetration front using a smaller particle size (10 nm) and three layers of Nano-SiO_2 at 12.5 % (300 g/cm^2).

3.5. Resistivity

Referring to Fig. 9, D-samples with either geometry have a higher resistivity than the respective C-samples, but the difference is greatest for those with the rectangular cross-section. In fact, rectangular cross-section D-samples had 44 % greater resistivity than comparable C-samples while D-samples with a circular cross-section had only 31 % greater resistivity than comparable C-samples. This finding is undoubtedly due to the larger overall cross-section of the rectangular geometry samples meaning that these had a larger area exposed to biodeposition. Lower resistivity in concrete is associated with greater susceptibility to corrosion of steel reinforcement elements, indeed, according to a study by Jalal et al. [59], resistivity of 120 Ωm is a key indicator with values above this indicating a reduced susceptibility to corrosion and values below this indicating the opposite. As can be seen in Fig. 9, all D-samples have resistivities in excess of this 120 Ωm benchmark and thus steel rebar corrosion would be unlikely.

Other work has also found increases in resistivity for concrete treated with silicon-based protective coatings. A study by M. Sanchez et al. [24], saw a trend to increased resistivity in concrete coated with Nano-SiO_2 with 7 nm particles at a concentration of 29 %. A previous study by M. Sanchez et al. [60] compared the same colloidal Nano-SiO_2 solution (29 %-7nm) with another comprising 12 nm particles at 37 % concentration. Results demonstrated that the greatest increase in resistivity was produced by the 29 %, 7 nm solution suggesting that both concentration and particle size affect the coating's ability to seal concrete pores.

3.6. Analysis of biogenic silica and surface microstructure

Micrographs and energy dispersive X-ray spectra for C- and D-samples are shown in Fig. 10a and b respectively. EDX analysis of the D-sample (lower image, Fig. 10b) shows two strong peaks corresponding to oxygen and silicon confirming that, as expected, the biodeposited film is mainly composed of silica (SiO_2). Comparing the micrographs showing the surface features of C-and D-samples (upper images in Fig. 10a and b respectively), it is possible to observe how the diatom biodeposited silica

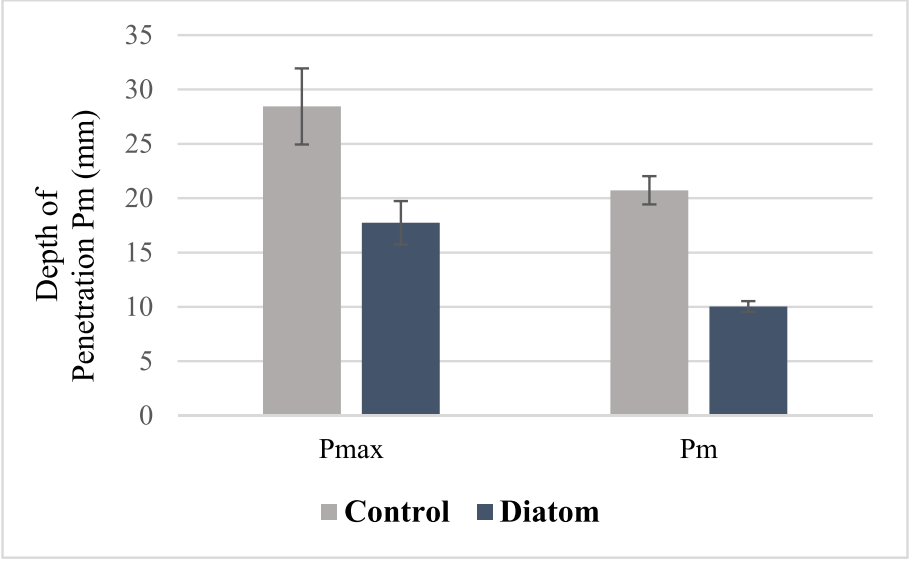

Fig. 8. Results for water depth: a) Maximum water depth P_{max} and B) Average water Depth $P_{m.}$

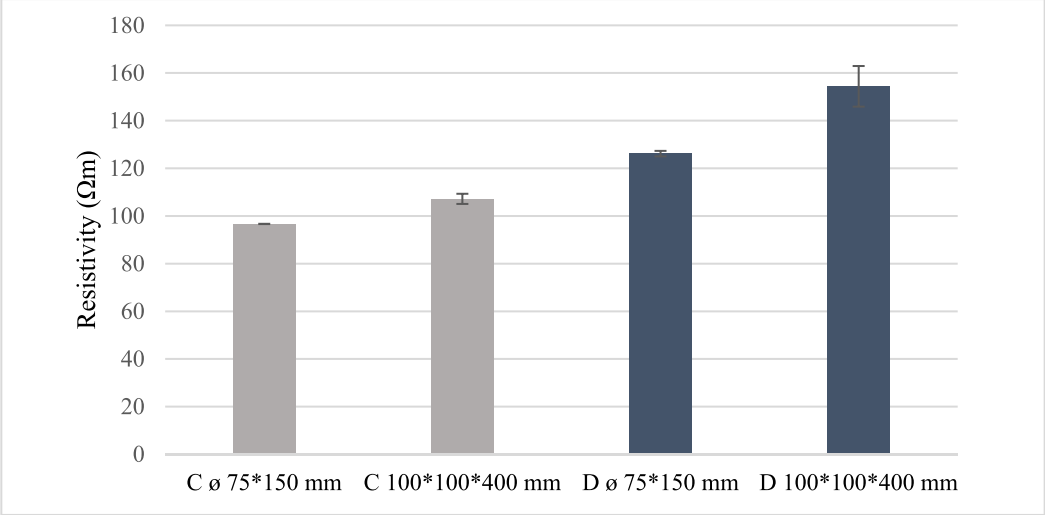

Fig. 9. Resistivity Results for Different Sample Geometries.

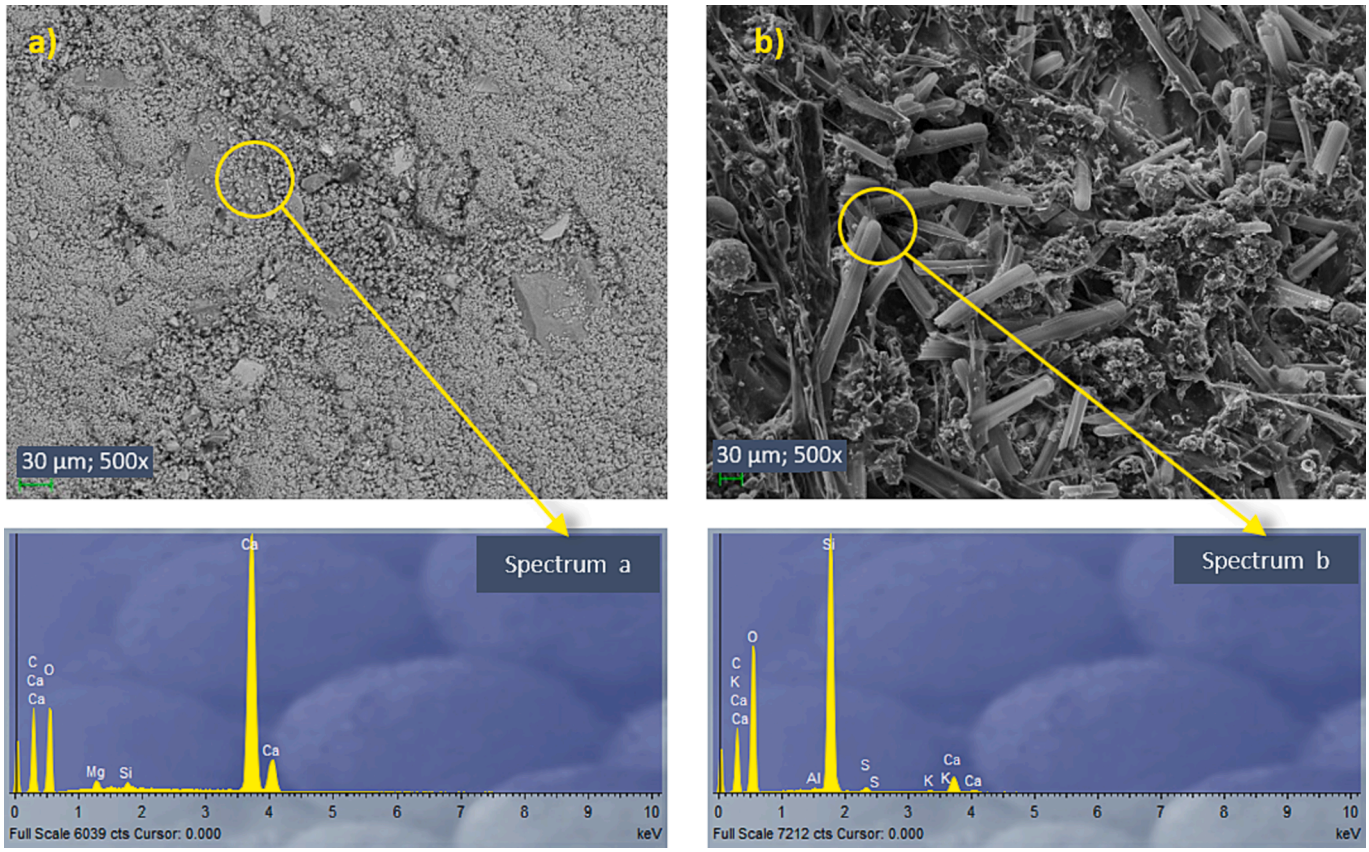

Fig. 10. Comparative Surface Microstructure and EDX Spectra of Compositions: (a) Control Sample and (b) Diatom Sample.

has filled and blocked the pores in the concrete substrate.

SEM examination the biofilms (Fig. 11) reveals considerable non-uniformity in the densities of diatoms attached to the substrate. This is because diatoms have a tendency to migrate to areas that offer the best environmental conditions for survival such as pores and surface niches that can provide protection from hydrodynamic shear forces that would otherwise limit diatom attachment and growth rate [37]. This phenomenon can be seen clearly in Fig. 11a, where diatoms are seen accumulating inside a surface pore in the concrete substrate. Fig. 11b is a further magnified image of a section of Fig. 11a allowing a more detailed analysis of the biofilm. Diatoms anchor themselves to surfaces by the secretion of the natural sealant, extracellular polymeric substance (EPS), and in the micrograph, it is possible to see how diatoms of various sizes (8–150 µm) accumulate on top of older deposits, producing overlapping layers to form large mats of fused material.

It is thought that SiO_2 protective coatings produce their effects due to the way they alter the microstructure of the concrete surface, specifically, reducing pore size and decreasing the interconnectivity between surface pores [19]. Ardalan et al. [58], for instance, observed that the application of Nano-SiO_2 to the surface of concrete resulted in a clear

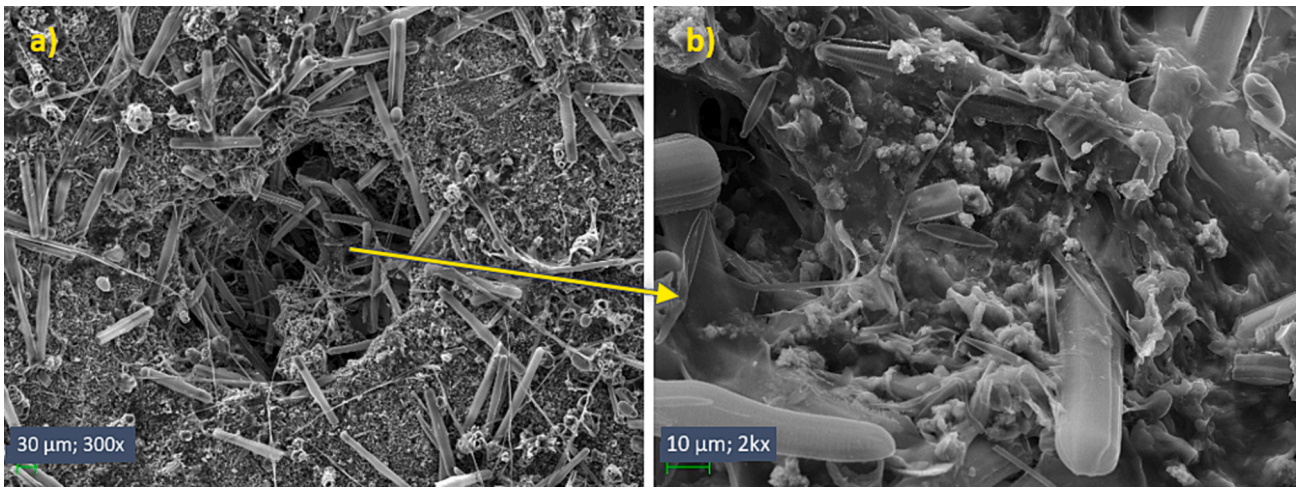

Fig. 11. SEM images of the surface microstructure of the biofilm: (a) Image showing the pore sealing; (b) Image showing different sizes of diatoms and multiple layers of biodeposition.

decrease in the size of the surface pores and even the complete sealing of some of them. A similar effect was observed in the study of Shirzadi Javid et al. [53], which demonstrated the use of silica nanoparticles to create a more compact surface microstructure. As our results show (Fig. 10 and 11), these phenomenon also appear to occur with biodeposited films: the adherence of diatoms to surface features of the concrete fills and blocks pores and this explains the improvements in concrete durability observed in this study.

4. Conclusions

This study presents an investigation into the effectiveness of a diatom biodeposited silica film as a treatment to improve the strength and durability of 50 % RA concrete. Samples of biofilm-treated concrete were compared to untreated samples subject to the main agents of environmental degradation of clean-water hydraulic concrete structures and the following conclusions can be drawn:

- Compressive strength tests show that the biodeposition process does not affect the mechanical properties of 50 % RA concrete. Indeed, results show a small increase in strength for biofilm-treated concrete compared to untreated samples. This increase is attributed to the fact that the biofilm formed has conferred a higher densification of the surface matrix of the concrete. This was achieved by the filling effect of the surface pores by the diatom frustules. Consequently, the structure of the treated concrete exhibits increased compactness and improved compressive strength, suggesting a positive effect of biodeposition on the quality of the material.
- Diatom biodeposition significantly reduces the carbonation rate of 50 % RA concrete. This phenomenon confers an effective impermeability of the concrete to gases. In addition, the depth of the penetration front is decreased by 56 % for biofilm-treated samples compared to untreated samples. These findings suggest that the biofilm can contribute to the long-term durability and strength of concrete, by reducing the rate of carbonation and limiting the penetration of gases into the material, this technique shows great potential for protecting concrete structures with high RA content.
- Biofilm-treated samples perform better than untreated samples in the freeze–thaw cycle test, specifically, biofilm-treated samples show a 26 % lower mass loss compared to controls after 28 freeze–thaw cycles. This suggests that the biofilm effectively limits the amount of water that can enter the concrete through surface pores thus reducing the damage caused due to ice-crystal formation.
- In tests of water penetration under pressure, biofilm-treated concrete demonstrates a 37 % reduction in maximum water penetration depth compared to untreated samples. In addition, the average water penetration depth for biofilm-treated samples is 57 % less than in untreated samples. This latter result is perhaps a more representative measure of biofilm effectiveness and demonstrates that this treatment can significantly reduce the permeability of 50 % RA concrete.
- The electrical resistivity tests show increases of 44 % for biofilm-treated samples compared to untreated samples. This effect varies according to the geometry of the specimens, being more evident in the rectangular cross-section specimens, due to their larger surface area exposed to biodeposition by sealing the concrete pores. This increased resistivity for treated samples demonstrates that biodeposition could provide effective protection against the corrosion of steel reinforcement elements so contributing to the longevity of concrete structures used in clean-water applications.
- SEM micrographs reveal that while the diatom biodeposited film is non-homogeneous due to its biological origin, the frustules adhering to the concrete substrate filled surface pores and formed a multilayered covering across the concrete surface. This adequately explains the improvements in durability observed in the study results.

As a final conclusion, the results indicate that a highly effective treatment of a biological nature can be achieved in a short period of time, only 3 months of immersion of the concrete in favourable environmental conditions. This immersion time is optimal during times when environmental conditions are favourable with positive photoperiods for diatom growth.

This finding shows the feasibility and rapidity of applying diatoms biodeposited silica to improve the properties of concrete. However, it is important to note that the effectiveness of this treatment may depend on local environmental conditions and the time of year when immersion takes place. Therefore, its practical implementation will require consideration of project-specific environmental and geographical factors.

In addition, in comparison to untreated concrete, biofilm-treated samples have increased resistance to carbonation, freeze–thaw cycles, water penetration under pressure and increased electrical resistivity demonstrating a reduced propensity to corrosion. These results suggest that biofilm protection could result in significant improvement in concrete durability without affecting the mechanical behaviour of concrete. These findings are ultimately consistent with previous research on silica-based protective coatings synthesised in the laboratory and suggest that concentration and particle size are important factors in the ability of

coatings to seal the pores of concrete. This would reduce the amount of raw materials required for the repair and maintenance of concrete structures in contact with clean water. In addition, biogenic silica is more environmentally friendly compared to other comparable treatments currently in use.

At present, research into bio-treatments for concrete, and particularly the use of diatom biodeposition, is scarce; however, this area of research is highly necessary to promote sustainability and improve the durability of concrete structures used in clean-water applications. The results presented in this study are very promising and suggest the need for further research in this field.

CRediT authorship contribution statement

Daniel Merino-Maldonado: Writing – original draft, Software, Methodology, Investigation, Formal analysis, Data curation. **Andrea Antolín-Rodríguez:** Methodology, Investigation, Data curation. **Saúl Blanco:** Supervision, Methodology, Investigation, Data curation. **Julia Mª Morán-del Pozo:** Writing – review & editing, Resources, Formal analysis. **Julia García-González:** Writing – review & editing, Resources, Formal analysis. **Andrés Juan-Valdés:** Writing – review & editing, Writing – original draft, Supervision, Conceptualization.

Declaration of Competing Interest

The authors declare that they have no known competing financial interests or personal relationships that could have appeared to influence the work reported in this paper.

Data availability

Data will be made available on request.

Acknowledgements

The authors are grateful for the grants awarded by the Junta de Castilla y León to finance the pre-doctoral hiring of research personnel, co-financed by the European Social Fund resolved in the ORDEN EDU/601/2020, (D.M.M.) and the ORDER EDU/875/2021 (A.A.R). The technical and human support provided by the CICT of the University of Jaén (UJA, MINECO, Junta de Andalucía, FEDER) and A. Olenici of the Electron Microscopy Unit of the University of Jaén (Spain) for kindly providing the SEM images is gratefully acknowledged.

References

[1] X.D. Wang, D.Y. Xu, W.X. Zhu, A.M. Deng, Z.B. Wang, Damage of concrete dams and its simulation calculation, Key Eng. Mater. 302–303 (2006) 624–629, https://doi.org/10.4028/www.scientific.net/kem.302-303.624.

[2] A. Banerjee, D.K. Paul, A. Acharyya, Optimization and safety evaluation of concrete gravity dam section, KSCE J. Civ. Eng. 19 (2015) 1612–1619, https://doi.org/10.1007/s12205-015-0139-0.

[3] A.T.M. Marsh, A.P.M. Velenturf, S.A. Bernal, Circular Economy strategies for concrete: implementation and integration, J. Clean. Prod. 362 (2022), 132486, https://doi.org/10.1016/j.jclepro.2022.132486.

[4] Z. Guo, A. Tu, C. Chen, D.E. Lehman, Mechanical properties, durability, and life-cycle assessment of concrete building blocks incorporating recycled concrete aggregates, J. Clean. Prod. 199 (2018) 136–149, https://doi.org/10.1016/j.jclepro.2018.07.069.

[5] X. He, Z. Zheng, M. Ma, Y. Su, J. Yang, H. Tan, Y. Wang, B. Strnadel, New treatment technology: the use of wet-milling concrete slurry waste to substitute cement, J. Clean. Prod. 242 (2020), 118347, https://doi.org/10.1016/j.jclepro.2019.118347.

[6] F. López-Gayarre, P. Serna, A. Domingo-Cabo, M.A. Serrano-López, C. López-Colina, Influence of recycled aggregate quality and proportioning criteria on recycled concrete properties, Waste Manag. 29 (2009) 3022–3028, https://doi.org/10.1016/j.wasman.2009.07.010.

[7] N. Makul, Cost-benefit analysis of the production of ready-mixed high-performance concrete made with recycled concrete aggregate: a case study in Thailand, Heliyon. 6 (2020) e04135.

[8] A. Juan-Valdés, D. Rodríguez-Robles, J. García-González, M.I. Sánchez de Rojas Gómez, M. Ignacio Guerra-Romero, N. De Belie, J.M. Morán-del Pozo, Mechanical and microstructural properties of recycled concretes mixed with ceramic recycled cement and secondary recycled aggregates. a viable option for future concrete, Constr. Build. Mater. 270 (2021), https://doi.org/10.1016/j.conbuildmat.2020.121455.

[9] P. Jagadesh, A. Juan-Valdés, M.I. Guerra-Romero, J.M. Morán-Del Pozo, J. García-González, R. Martínez-García, Effect of design parameters on compressive and split tensile strength of self-compacting concrete with recycled aggregate: an overview, Appl. Sci. 11 (2021) 6028, https://doi.org/10.3390/app11136028.

[10] J. Kim, Influence of quality of recycled aggregates on the mechanical properties of recycled aggregate concretes: an overview, Constr. Build. Mater. 328 (2022), 127071, https://doi.org/10.1016/j.conbuildmat.2022.127071.

[11] Z.J. Grdic, G.A. Toplicic-Curcic, I.M. Despotovic, N.S. Ristic, Properties of self-compacting concrete prepared with coarse recycled concrete aggregate, Constr. Build. Mater. 24 (2010) 1129–1133, https://doi.org/10.1016/j.conbuildmat.2009.12.029.

[12] D. Pedro, J. de Brito, L. Evangelista, Structural concrete with simultaneous incorporation of fine and coarse recycled concrete aggregates: mechanical, durability and long-term properties, Constr. Build. Mater. 154 (2017) 294–309, https://doi.org/10.1016/j.conbuildmat.2017.07.215.

[13] G. Dimitriou, P. Savva, M.F. Petrou, Enhancing mechanical and durability properties of recycled aggregate concrete, Constr. Build. Mater. 158 (2018) 228–235, https://doi.org/10.1016/j.conbuildmat.2017.09.137.

[14] A.A. Mikhasek, Y.M. Galitskova, O.A. Tutova, The use of crusher-run aggregates of reinforced concrete frames when reconstructing hydraulic structures, Procedia Eng. 153 (2016) 456–460, https://doi.org/10.1016/j.proeng.2016.08.156.

[15] X. Pan, Z. Shi, C. Shi, T.C. Ling, N. Li, A review on surface treatment for concrete – Part 2: performance, Constr. Build. Mater. 133 (2017) 81–90, https://doi.org/10.1016/j.conbuildmat.2016.11.128.

[16] M. Sánchez, P. Faria, L. Ferrara, E. Horszczaruk, H.M. Jonkers, A. Kwiecień, J. Mosa, A. Peled, A.S. Pereira, D. Snoeck, M. Stefanidou, T. Stryszewska, B. Zając, External treatments for the preventive repair of existing constructions: a review, Constr. Build. Mater. 193 (2018) 435–452, https://doi.org/10.1016/j.conbuildmat.2018.10.173.

[17] Y.G. Zhu, S.C. Kou, C.S. Poon, J.G. Dai, Q.Y. Li, Influence of silane-based water repellent on the durability properties of recycled aggregate concrete, Cem. Concr. Compos. 35 (2013) 32–38, https://doi.org/10.1016/j.cemconcomp.2012.08.008.

[18] E. Franzoni, B. Pigino, C. Pistolesi, Ethyl silicate for surface protection of concrete: performance in comparison with other inorganic surface treatments, Cem. Concr. Compos. 44 (2013) 69–76, https://doi.org/10.1016/j.cemconcomp.2013.05.008.

[19] P. Hou, X. Cheng, J. Qian, S.P. Shah, Effects and mechanisms of surface treatment of hardened cement-based materials with colloidal nanoSiO2 and its precursor, Constr. Build. Mater. 53 (2014) 66–73, https://doi.org/10.1016/j.conbuildmat.2013.11.062.

[20] W. She, J. Yang, J. Hong, D. Sun, S. Mu, C. Miao, Superhydrophobic concrete with enhanced mechanical robustness: nanohybrid composites, strengthen mechanism and durability evaluation, Constr. Build. Mater. 247 (2020), 118563, https://doi.org/10.1016/j.conbuildmat.2020.118563.

[21] M.R. Sakr, M.T. Bassuoni, Silane and methyl-methacrylate based nanocomposites as coatings for concrete exposed to salt solutions and cyclic environments, Cem. Concr. Compos. 115 (2021), 103841, https://doi.org/10.1016/j.cemconcomp.2020.103841.

[22] K. Xia, Y. Gu, W. Jin, L. Jiang, K. Lü, M. Guo, Carbonation resistance of hybrid nanosio2 modified cementitious surface protection materials, J. Wuhan Univ. Technol. Mater. Sci. Ed. 37 (2022) 855–862, https://doi.org/10.1007/s11595-022-2607-y.

[23] T. Li, Y. Wu, H. Wu, A study on impact of different surface treatment agents on the durability of airport pavement concrete, Coatings 12 (2022) 1–21, https://doi.org/10.3390/coatings12020162.

[24] M. Sánchez-Moreno, J.L. García-Calvo, F. Tavares-Pinto, Colloidal nanosilica treatments for sealing cracks in mortar, Materials (basel). 15 (2022), https://doi.org/10.3390/ma15186338.

[25] R. Li, P. Hou, N. Xie, Z. Ye, X. Cheng, S.P. Shah, Design of SiO2/PMHS hybrid nanocomposite for surface treatment of cement-based materials, Cem. Concr. Compos. 87 (2018) 89–97, https://doi.org/10.1016/j.cemconcomp.2017.12.008.

[26] A. Chiovitti, T.M. Dugdale, R. Wetherbee, Diatom adhesives: molecular and mechanical properties, Biol. Adhes. 1 (2006) 79–103, https://doi.org/10.1007/978-3-540-31049-5_5.

[27] M. Terracciano, L. De Stefano, I. Rea, Diatoms green nanotechnology for biosilica-based drug delivery systems, Pharmaceutics. 10 (2018) 1–15, https://doi.org/10.3390/pharmaceutics10040242.

[28] E. Axtell III, G. Sakoske, D. Swiler, M. Hensel, M. Baumann, D. Matalka, G. Nuccetelli, Structured Self-Cleaning Suerfaces and Method of Forming Same, US 2006/0246277, 2006.

[29] EN 197-1. Cement. Part 1: Composition, specifications and conformity criteria for commo on cements; AENOR: Madrid, Spain, 2011.

[30] R. Martínez-García, I.M. Guerra-Romero, J.M. Morán-del Pozo, J. de Brito, A. Juan-Valdés, Recycling aggregates for self-compacting concrete production: a feasible option, Materials (basel) 13 (2020), https://doi.org/10.3390/ma13040868.

[31] R. Martínez-García, Evaluation of the use of recycled concrete aggregates for the production of self-compacting concretes and cement mortars, University of León, 2021.

[32] EN 933-1. Tests for geometrical properties of aggregates. Part 1: Determination of pa rticle size distribution. Sieving method; AENOR: Madrid, Spain, 2012.

[33] EN 1097-6. Tests for mechanical and physical properties of aggregates. Part 6: Determination of particle density and water absorption; AENOR: Madrid, Spain, 2014.

[34] EN 12620:2003+A1. Aggregates for concrete; AENOR: Madrid, Spain, 2009.
[35] A. Djerbi Tegguer, Determining the water absorption of recycled aggregates utilizing hydrostatic weighing approach, Constr. Build. Mater. 27 (2012) 112–116, https://doi.org/10.1016/j.conbuildmat.2011.08.018.
[36] EN 933-11. Tests for geometrical properties of aggregates. Part 11: Classification test for the constituents of coarse recycled aggregate; AENOR: Madrid, Spain, 2009.
[37] P.J. Molino, R. Wetherbee, The biology of biofouling diatoms and their role in the development of microbial slimes, Biofouling 24 (2008) 365–379, https://doi.org/10.1080/08927010802254583.
[38] W. Admiraal, Influence of light and temperature on the growth rate of estuarine benthic diatoms in culture, Mar. Biol. 39 (1976) 1–9, https://doi.org/10.1007/BF00395586.
[39] S. Lacoursière, I. Lavoie, M.A. Rodríguez, S. Campeau, Modeling the response time of diatom assemblages to simulated water quality improvement and degradation in running waters, Can. J. Fish. Aquat. Sci. 68 (2011) 487–497, https://doi.org/10.1139/F10-162.
[40] ISO 10260. Measurement of biochemical parameters. Spectrometric determination of the chlorophyll a concentration, London, United Kingdom, 1992.
[41] EN 13946.Water quality. Guidance for the routine sampling and preparation of benthic diatoms from rivers and lakes; AENOR: Madrid, Spain, 2014.
[42] EN 14407. Water quality. Guidance for the identification and enumeration of benthic diatom samples from rivers and lakes; AENOR: Madrid, Spain, 2015.
[43] G. Hofmann, M. Werum, H. Lange-Bertalot, Diatomeen im Süßwasser-Benthos von Mitteleuropa : Bestimmungsflora Kieselalgen für die ökologische Praxis ; über 700 der häufigsten Arten und ihre Ökologie, 2011.
[44] C. Lecointe', M. Coste, J. Prygiel, "Omnidia": software for taxonomy, calculation of diatom indices and inventories management, Hydrobiologia 269 (1993) 509–513.
[45] EN 12390-3 Testing hardened concrete. Part 3: Compressive strength of test specimens; AENOR: Madrid, Spain, 2020.
[46] EN 12390-10. Testing hardened concrete. Part 10: Determination of the carbonation resistance of concrete at atmospheric carbon dioxide levels Part 10: Determination of resistance to carbonation of concrete at atmospheric levels of carbon dioxide; AENOR: Madrid, Spain, 2019.
[47] R.V. Silva, R. Neves, J. De Brito, R.K. Dhir, Carbonation behaviour of recycled aggregate concrete, Cem. Concr. Compos. 62 (2015) 22–32, https://doi.org/10.1016/J.CEMCONCOMP.2015.04.017.
[48] EN 1339. Concrete paving flags. Requirements and test methods; AENOR: Madrid, Spain, 2004.
[49] EN 12390-8. Testing hardened concrete. Part 8: Depth of penetration of water under pressure; AENOR: Madrid, Spain, 2020.
[50] EN 12390-6. Testing hardened concrete. Part 6: Tensile splitting strength of test specimens; AENOR: Madrid, Spain, 2010.
[51] ImageJ. Computer Software, Version 1.8.0; National Institutes of Health, Bethesda, MD, USA. Available online: https://imagej.nih.gov/ij/ (accessed on 2023).
[52] EN 83988-1. Concrete durability. Test methods. Determination of the electrical resistivity. Part 1: Direct test (reference method); AENOR: Madrid, Spain, 2008.
[53] A.A. Shirzadi Javid, P. Ghoddousi, M. Zareechian, A. Habibnejad Korayem, Effects of spraying various nanoparticles at early ages on improving surface characteristics of concrete pavements, Int. J. Civ. Eng. 17 (2019) 1455–1468, https://doi.org/10.1007/s40999-019-00407-4.
[54] M. Elsalamawy, A.R. Mohamed, E.M. Kamal, The role of relative humidity and cement type on carbonation resistance of concrete, Alexandria Eng. J. 58 (2019) 1257–1264, https://doi.org/10.1016/j.aej.2019.10.008.
[55] W. De Muynck, D. Debrouwer, N. De Belie, W. Verstraete, Bacterial carbonate precipitation improves the durability of cementitious materials, Cem. Concr. Res. 38 (2008) 1005–1014, https://doi.org/10.1016/j.cemconres.2008.03.005.
[56] F.C. Meldrum, C. O'Shaughnessy, Crystallization in Confinement, Adv. Mater. 32 (2020), https://doi.org/10.1002/adma.202001068.
[57] Z. Liu, W. Hansen, Effect of hydrophobic surface treatment on freeze-thaw durability of concrete, Cem. Concr. Compos. 69 (2016) 49–60, https://doi.org/10.1016/j.cemconcomp.2016.03.001.
[58] R.B. Ardalan, N. Jamshidi, H. Arabameri, A. Joshaghani, M. Mehrinejad, P. Sharafi, Enhancing the permeability and abrasion resistance of concrete using colloidal nano-SiO2 oxide and spraying nanosilicon practices, Constr. Build. Mater. 146 (2017) 128–135, https://doi.org/10.1016/j.conbuildmat.2017.04.078.
[59] M. Jalal, E. Mansouri, M. Sharifipour, A.R. Pouladkhan, Mechanical, rheological, durability and microstructural properties of high performance self-compacting concrete containing SiO2 micro and nanoparticles, Mater. Des. 34 (2012) 389–400, https://doi.org/10.1016/j.matdes.2011.08.037.
[60] M. Sánchez, M.C. Alonso, R. González, Preliminary attempt of hardened mortar sealing by colloidal nanosilica migration, Constr. Build. Mater. 66 (2014) 306–312, https://doi.org/10.1016/j.conbuildmat.2014.05.040.